Evaluating Satellite-Based Diurnal Cycles of Precipitation in the African Tropics

UWE PFEIFROTH* AND JÖRG TRENTMANN

Department of Climate and Environment, Deutscher Wetterdienst, Offenbach am Main, Germany

ANDREAS H. FINK

Institute for Meteorology and Climate Research, Karlsruhe Institute of Technology, Karlsruhe, Germany

BODO AHRENS

Institute for Atmospheric and Environmental Sciences, Goethe University, Frankfurt am Main, Germany

(Manuscript received 4 March 2015, in final form 26 July 2015)

ABSTRACT

Precipitation plays a major role in the energy and water cycles of the earth. Because of its variable nature, consistent observations of global precipitation are challenging. Satellite-based precipitation datasets present an alternative to in situ–based datasets in areas sparsely covered by ground stations. These datasets are a unique tool for model evaluations, but the value of satellite-based precipitation datasets depends on their application and scale. Numerous validation studies considered monthly or daily time scales, while less attention is given to subdaily scales. In this study subdaily satellite-based rainfall data are analyzed in West Africa, a region with strong diurnal variability. Several satellite-based precipitation datasets are validated, including Tropical Rainfall Measuring Mission (TRMM) Multisatellite Precipitation Analysis (TMPA), TRMM 3G68 products, Precipitation Estimation from Remotely Sensed Information Using Artificial Neural Networks (PERSIANN), and Climate Prediction Center (CPC) morphing technique (CMORPH) data. As a reference, highly resolved in situ data from the African Monsoon Multidisciplinary Analysis–Couplage de l'Atmosphere Tropical et du Cycle Hydrologique (AMMA-CATCH) are used. As a result, overall the satellite products capture the diurnal cycles of precipitation and its variability as observed on the ground reasonably well. CMORPH and TMPA data show overall good results. For locally induced convective rainfall in the evening most satellite data show slight delays in peak precipitation of up to 2 h.

1. Introduction

In meteorology and climatology the spatial and temporal variability of precipitation is of great importance. The key to further understanding precipitation variability at various spatial and temporal scales is having the best possible precipitation database available. Especially in the tropics, which globally receive maximum rainfall, precipitation plays a major role for scientific analysis, but it is also of high relevance for the economy and society as a whole. Large tropical and subtropical regions like India, East Asia, or West Africa are affected by monsoon systems, which are responsible for rainy seasons. Even though those rainfall events may cause severe flooding, they are essential for human life. The tropical monsoon systems do not only exhibit annual and seasonal variability, but are also subject to large diurnal variations (e.g., Lau et al. 2007; Kikuchi and Wang 2008). Heavy rainfall usually falls in convective events, which poses a challenge for observations and modeling. The diurnal cycle of precipitation systematically impacts atmospheric properties like humidity and temperatures (e.g., through evaporation) and therefore is a prominent feature of the tropical climate (Yang and Slingo 2001).

Denotes Open Access content.

* Additional affiliation: Institute for Atmospheric and Environmental Sciences, Goethe University, Frankfurt am Main, Germany.

Corresponding author address: Uwe Pfeifroth, Deutscher Wetterdienst, Frankfurter Staße 135, 63067 Offenbach am Main, Germany.
E-mail: uwe.pfeifroth@dwd.de

DOI: 10.1175/JAMC-D-15-0065.1

Unfortunately, there is a lack of ground-based meteorological measurements in parts of the earth and in particular in tropical regions. The sparse distribution of rain gauge stations in the tropics and the lack of a dense measuring network are problematic because of the high spatiotemporal variability of tropical precipitation. In recent years efforts have been made to retrieve precipitation estimates through remote sensing from satellites to fill the gaps in the station network. Tapiador et al. (2012) and Kidd and Levizzani (2011) give thorough overviews on currently available satellite-based precipitation datasets. These datasets are unique in delivering precipitation with quasi-global spatiotemporal coverage, which make these datasets valuable for increasing our knowledge of precipitation distribution and variability (Kucera et al. 2013). Satellite-based high-resolution precipitation datasets are commonly used to study precipitation diurnal cycles (e.g., Sato et al. 2009; Dirmeyer et al. 2012; Birch et al. 2014; Pohl et al. 2014). Moreover, these datasets are an important tool for evaluating precipitation as simulated by numerical weather prediction and climate models, which often have deficiencies in modeling precipitation (e.g., Dobler and Ahrens 2008; Sato et al. 2009; Kothe et al. 2014). Concerning subdaily variability, models still have difficulties in simulating the proper timing and size of the precipitation diurnal cycles because of the necessity to parameterize small-scale processes (Dirmeyer et al. 2012). Recently, however, Bechtold et al. (2014) substantially improved the diurnal cycle of precipitation in the global model of the European Centre for Medium-Range Weather Forecasts by improved parameterizations with reference to, among others, Tropical Rainfall Measuring Mission (TRMM) satellite data in Africa. Satellite-based precipitation datasets can help to further identify and understand model deficiencies.

Even though there has been progress in developing satellite-based precipitation datasets in recent years, it is problematic to use them unevaluated as reference for any purpose. It is challenging to correctly estimate precipitation reaching the ground by means of satellite remote sensing, as it is not a direct measurement and relies on assumptions like temperature profiles or droplet sizes. Moreover, the data quality is dependent on the precipitation regime. Data uncertainties at a certain location have to be expected because of the algorithm itself but also owing to the limited spatiotemporal coverage (Negri et al. 2002a; Kidd and Levizzani 2011; Pfeifroth et al. 2013). The latter is especially problematic for tropical regions often affected by convective rainfall events (Yang and Slingo 2001). Weak temporal coverage may reduce data quality, especially when looking at subdaily rainfall variability. To overcome this deficiency, efforts have been made to improve the spatiotemporal coverage by combining data from different satellites into merged products (Kidd and Levizzani 2011). In particular, these datasets make use of infrared measurements by geostationary satellites to improve the spatiotemporal sampling of low-earth-orbiting satellites. But precipitation estimates based on infrared measurements are more indirect and hence more uncertain than those based on microwave measurements. Overall, it is known that precipitation estimates by satellites perform better in the tropics than in high latitudes, as described by Ebert et al. (2007). This is due to the fact that tropical precipitation is mostly convective, which implies a clearer signal in satellite measurements as a result of heavy rainfall from thick clouds rather than precipitation from shallow clouds. The difficulties involved with accounting for the time lag between maximum rainfall and the maximum development of a convective cloud have already been addressed by Reed and Jaffe (1981). This is still one of the issues that infrared (IR)-based rainfall algorithms have to deal with. Nevertheless, thanks to the incorporation of high-resolution IR data, current satellite-based precipitation datasets deliver their observations at 3-hourly (or even higher) temporal resolution. As a result of the fact that high-resolution reference data are very rare in tropical regions, systematic validations of subdaily variations as provided by satellite-based precipitation data are infrequent.

Various studies have evaluated satellite-based precipitation datasets on different scales. Different satellite-based precipitation datasets are intercompared to check their consistency and to reveal deficiencies, as has been done by Andersson et al. (2011). Some studies used rain gauge data to evaluate differences between the ground-truth and satellite-based precipitation estimates (e.g., Pfeifroth et al. 2013). Usually it is monthly or daily means that are considered, while some studies also validated subdaily data. Sapiano and Arkin (2009) evaluated different high-resolution satellite-based datasets, including TRMM Multisatellite Precipitation Analysis (TMPA) and Climate Prediction Center (CPC) morphing technique (CMORPH) data, with rain gauge data and found correlations of about 0.5 for 3-hourly data in the southern United States and concluded that CMORPH is best suited to studying precipitation variability. Janowiak et al. (2005) evaluated one summer season of CMORPH precipitation diurnal cycles with weather radar data for the United States and found reasonable agreement for the mean diurnal cycle.

Thanks to the African Monsoon Multidisciplinary Analysis–Couplage de l'Atmosphere Tropical et du Cycle Hydrologique (AMMA-CATCH) project, some longer-term high-resolution rain gauge data are now available, which are used as a precipitation reference for the African tropical climate in this study. Also Roca et al. (2010) and Gosset et al. (2013) used station data provided by the AMMA database for West Africa to validate different satellite-based and rain gauge–based datasets in West Africa. By comparison with the AMMA data, Roca et al. (2010) concluded that TMPA data are the best suited for analyzing diurnal cycles. Gosset et al. (2013) found temporal correlations between satellite estimates and rain gauge data in the range of 0.5–0.7 for daily time steps. He et al. (2015) used TMPA and AMMA station data to improve model simulations in West Africa and also evaluated the diurnal cycle of rainfall. They found a pronounced evening peak and a weaker morning peak for 2005. Sane et al. (2012) analyzed the diurnal cycle of precipitation in Senegal in two months of 2006 using rain gauge and TMPA satellite data and found a secondary peak of rainfall in the morning.

In this study we provide information on the ability of state-of-the-art high-resolution satellite-based precipitation datasets to observe systematic diurnal variations. Therefore, we evaluate, overall, seven different satellite-based precipitation products with at least 3-hourly temporal resolution with reference to in situ observations in the African tropics. We focus on the mean diurnal cycles of precipitation and also analyze its mean month-to-month and year-to-year variability. We used rain gauge data from the AMMA-CATCH station network to evaluate satellite-based precipitation datasets including the TMPA, the TRMM 3G68 datasets, two CMORPH datasets, and the Precipitation Estimation from Remotely Sensed Information using Artificial Neural Networks (PERSIANN). In sections 2 and 3 we describe the data and the methods used. The evaluation results are presented and discussed in sections 4 and 5.

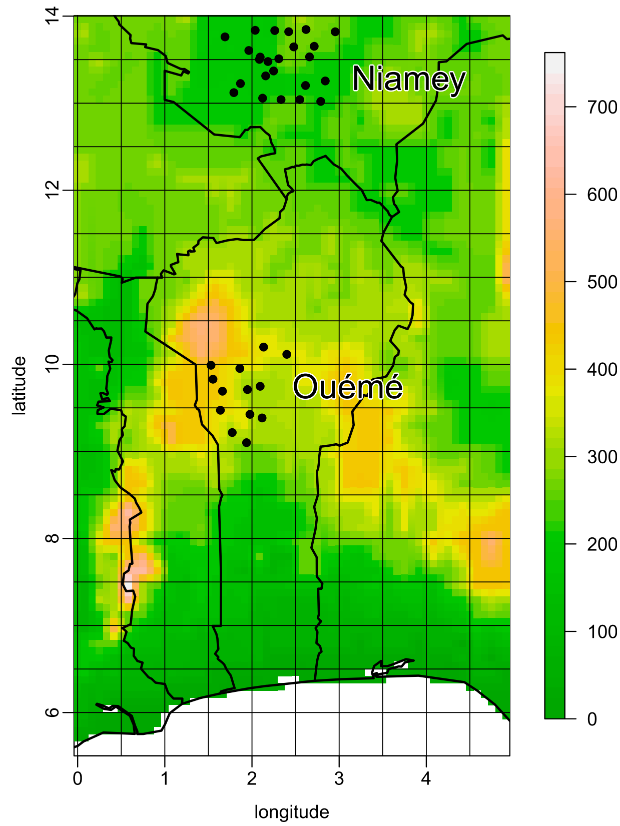

FIG. 1. Topographic map of the analysis region in West Africa, including the AMMA stations used at the Niamey (northern) and Ouémé (southern) mesosites.

2. Data

a. *AMMA rain gauge data*

The African Monsoon Multidisciplinary Analysis project is an international interdisciplinary program dealing with the West African monsoon, its variability, and its impacts on human life. Within the AMMA project, three so-called mesosites with enhanced surface measurements were set up, two of which were the Ouémé mesosite in central Benin and the Niamey mesosite in southern Niger (Lebel et al. 2010). Within these two sites rain gauge networks were maintained until recently by the Institut de Recherche pour le Développement (IRD) funded AMMA-CATCH program. Rainfall data at high temporal resolution and for more than a decade are freely available from the AMMA-CATCH database (see http://www.amma-catch.org; data accessed in June 2015).

Overall, we used hourly observations from 37 stations covering the monsoon seasons (May–September) during the time period 2000–11. The chosen stations are mainly located in the Ouémé mesosite in Benin and in the Niamey mesosite in Niger (see Fig. 1). The two mesosites have different rainfall characteristics (Gosset et al. 2013) and are therefore analyzed separately in this study. We use the AMMA-CATCH station data as the reference to validate the satellite products. Therefore, the stations have been gridded as described in section 3.

b. *TRMM 3G68 dataset*

The Tropical Rainfall Measuring Mission is a joint venture between the National Aeronautics and Space Administration and the Japan Aerospace Exploration Agency designed to monitor and study tropical precipitation. The TRMM satellite covers the area from 35°N to 35°S; its sensor package is described in Kummerow et al.

(1998). The TRMM satellite's orbit is circular and non-sun-synchronous, which means that each location is covered at different local times each day. This makes the TRMM satellite especially interesting for analyzing the diurnal cycle of precipitation.

The TRMM 3G68 dataset in version 7 is used, which consists of three different products based on two different instruments aboard the TRMM satellite. Product 2A12 is based on the TRMM Microwave Imager (TMI), 2A25 is based on the TRMM Precipitation Radar (PR), and the 3B31 product is a combination of the 2A12 and 2A25 products and is referred to as TRMM-COMB in the following. All TRMM 3G68 products consist of 1-hourly instantaneous rainfall estimates gridded to a 0.5° × 0.5° grid and cover the global tropics (40°N–40°S).

The PR sensor is an active instrument and delivers the most direct measure of precipitation, which implies that the PR should give the best measure of precipitation. Contrary to the PR, the TMI sensor is a passive microwave imager that relies on emission and scattering signals due to precipitation-sized particles. The TMI sensor swath is wider than that of the PR, but its measure of precipitation is more indirect. TRMM-COMB combines TMI-calibrated brightness temperatures and PR reflectivities to generate a best-of-TRMM-only product at the instantaneous time scale. The TRMM-COMB algorithm is designed to make use of the strengths of both sensors (Haddad et al. 1997). A drawback of the TRMM-only datasets is its limited spatiotemporal sampling, as analyzed by Negri et al. (2002b). On average, the 1-hourly PR and TMI version-7 datasets on the 0.5° × 0.5° grid are based on 13–15 and 37–40 overpasses per month in the target region, respectively. To improve the spatiotemporal coverage, we aggregated the 1-hourly instantaneous TRMM G68 data to 3-hourly data by averaging. This is close to the ideal aggregation interval of 4 h, as proposed by Negri et al. (2002b).

c. TRMM 3B42 dataset

The TRMM 3B42 dataset in version 7 is a multi-satellite precipitation dataset. It incorporates numerous different satellite sources including microwave and infrared sensor data from polar-orbiting and geostationary satellites (Huffman and Bolvin 2007) into a final product on a 0.25° × 0.25° grid. The algorithm for generating the TRMM 3B42 dataset consists of three main steps. First, the TRMM-COMB (cf. section 2b) product is used to calibrate the different microwave data sources. Then, the infrared-based datasets are converted into precipitation estimates using the calibrated microwave data. Finally, the microwave and infrared data are merged into 3-hourly precipitation estimates.

d. CMORPH technique datasets

The Climate Prediction Center morphing technique developed by the National Oceanic and Atmospheric Administration produces a quasi-global precipitation dataset with high spatiotemporal resolution. This technique uses precipitation estimates derived from passive microwave observations and transports these estimates via spatial propagation information obtained from geostationary satellite IR data (Joyce et al. 2004). The morphing technique makes use of 30-min-resolution IR data to propagate and morph the microwave precipitation estimates. It not only transports the spatial rainfall features but also interpolates the rainfall intensities both forward and backward in time to get the best estimate. These precipitation estimates are available in a very high resolution of 30 min in time and 8 km in space, corresponding to the resolution of the geostationary IR data used. A lower-resolution CMORPH data version is available as 3-hourly averaged precipitation estimates, on a 0.25° × 0.25° grid. Both datasets are provided online (http://rda.ucar.edu). In this study we are using both the lower- and higher-resolution CMORPH version-1.0 data, referred to as CMORPH and CMORPH-hq, respectively.

e. PERSIANN dataset

The Precipitation Estimation from Remotely Sensed Information using Artificial Neural Networks dataset is an effort coordinated by the Center for Hydrometeorology and Remote Sensing (CHRS) of the University of California (Sorooshian et al. 2000; Ashouri et al. 2015). PERSIANN data are available 3 hourly on a 0.25° × 0.25° grid. To generate the PERSIANN precipitation data, IR measurements from global geostationary IR composites are used to estimate precipitation by applying a neural network trained with various passive microwave based precipitation estimates. The data and more information are available online (http://chrs.web.uci.edu/persiann).

f. CLAAS dataset

The Cloud Property Dataset using SEVIRI (CLAAS) is generated within the EUMETSAT Satellite Application Facility on Climate Monitoring (CM SAF) (Stengel et al. 2014). The CM SAF generates and provides datasets on various essential climate variables with a focus on the earth's energy cycles. The CLAAS dataset contains several cloud property parameters including cloud-top information at high spatial and temporal resolutions. The dataset is well suited to study diurnal cycles (Kniffka et al.

2014). We used 1-hourly monthly mean diurnal cycles of cloud-top temperatures (CTT) during a 4-yr period for the three central monsoon months of June–August. CLAAS is used in this study to analyze the correspondence of diurnal cycles of rainfall and cloud-top temperatures.

3. Methods

We are using hourly rain gauge data in West Africa as obtained from the AMMA-CATCH database as ground-based reference when comparing with different gridded precipitation datasets during the time period 2000–11. The AMMA-CATCH station data have proven to be of reasonable quality, especially when aggregating in space and time, for example, to 1° daily data (Gosset et al. 2013). While setting up the validation, we were facing the issue of different datasets having different spatiotemporal resolutions. Further, the difficulty of comparing point data to gridded data is addressed by spatial and temporal averaging.

As the AMMA-CATCH stations used are distributed relatively densely in some areas, multiple stations could be merged into grid boxes. The stations were aggregated into grid boxes with a size of $0.5° \times 0.5°$ by averaging the respective stations located in the same grid box. By doing so, the problem of station representativeness could be reduced. All the satellite datasets are also analyzed on the same $0.5° \times 0.5°$ grid. The regridding, if necessary, was performed by conservative remapping. We thereby also aggregated the 1-hourly instantaneous TRMM G68 data into 3-hourly data to be in line with the other satellite data and to account for the lower sampling rate. This brings the TRMM 3G68 data close to the ideal aggregation interval of 4 h, as proposed by Negri et al. (2002a).

Further improvement of the station data representativeness is achieved by temporal averaging. First, the monthly mean diurnal cycles for each grid box are computed by averaging the rainfall amounts for the individual hours. These monthly diurnal cycles are then further regionally averaged and then further averaged to multiyear monthly diurnal cycles (see Figs. 5 and 6), to multimonth yearly diurnal cycles (see Figs. 3 and 4), and to overall mean diurnal cycles (see Fig. 2). Especially when comparing station data and gridded data at smaller temporal scales than in this study, one should explicitly account for the temporal and spatial sampling errors, as proposed, for example, by Kirstetter et al. (2013) and Roca et al. (2010).

Moreover, we have to consider that the different datasets not only have different spatial resolutions but

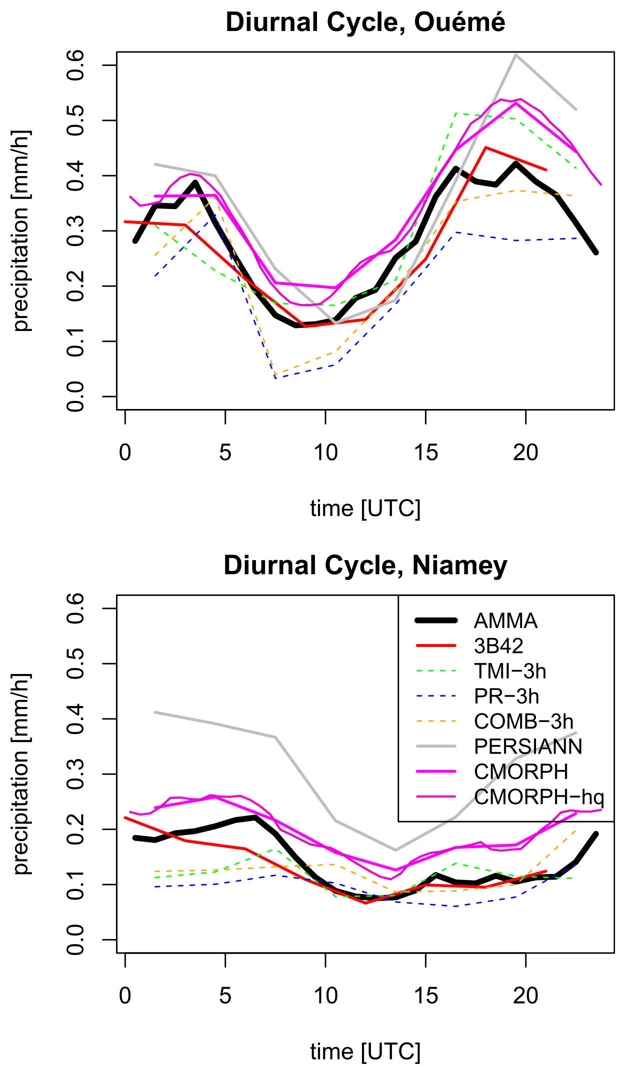

FIG. 2. Mean diurnal cycles of the satellite-based datasets and the AMMA-CATCH data at the (top) Ouémé and (bottom) Niamey mesosites during the monsoon season (MJJAS).

also different temporal resolutions. As the analyzed datasets are mostly incorporating multiple satellites, the individual single-sensor-based estimates are usually aggregated and finally averaged over a certain time interval during data processing. Accounting for those aggregating time intervals is necessary to compare the actual diurnal timings of precipitation. For the validation of the mean diurnal cycles we used the satellite data at 3-hourly temporal resolution and the AMMA-CATCH reference at hourly resolution. The CMORPH-hq satellite dataset was kept in its native temporal resolution of 30 min to check if there is an added value on the standard CMORPH dataset. A summary of the datasets used, including relevant information on the resolutions, is given in Table 1.

TABLE 1. Spatial and temporal resolutions and time stamp information of all data used as given by the data provider and as used in the validation.

	AMMA	TRMM 3B42	PR	TMI	TRMM-COMB	PERSIANN	CMORPH	CMORPH-hq
Native resolution								
Spatial (lat–lon)	—	0.25°	0.5°	0.5°	0.5°	0.25°	0.25°	8 km
Temporal	1-hourly	3-hourly	1-hourly	1-hourly	1-hourly	3-hourly	3-hourly	30 min
Time stamp	End	Central	Beginning	Beginning	Beginning	Beginning	Beginning	Beginning
Resolution used for the validation								
Spatial (lat–lon)	0.5°	0.5°	0.5°	0.5°	0.5°	0.5°	0.5°	0.5°
Temporal	1-hourly	3-hourly	3-hourly	3-hourly	3-hourly	3-hourly	3-hourly	30 min
Time stamp	Central	Central	Central	Central	Central	Central	Central	Central

In most of the analyzed satellite datasets the time stamp given in the data corresponds to the starting point of the accumulation interval (see Table 1). In the TRMM 3B42 dataset each 3-hourly precipitation value given at a certain UTC time corresponds to the mean precipitation estimated in the interval of ±1.5 h relative to the time stamp. The time stamps of all other satellite-based datasets have been adjusted to represent the central time of the summation interval. Thereby, we account for the different starting points of the aggregation intervals. The data are evaluated on the common 0.5° × 0.5° grid.

The evaluation focuses on two main characteristics of the diurnal cycle of precipitation: the diurnal timing of the maximum precipitation value and the size of the diurnal peaks. The analysis is limited to the monsoon season defined as the five months of May, June, July, August, and September, when, except for the coastal strip along the Guinea coast, the majority of the annual rainfall occurs in West Africa. The results are separately shown for the Niamey and Ouémé mesosites, as well as its month-to-month and year-to-year variability. Especially when analyzing the diurnal cycle for individual years, larger uncertainties occur as a result of the shorter averaging interval, visible by a larger scatter and a less smooth diurnal cycle.

At the Ouémé mesosite two diurnal rainfall peaks were found, which are analyzed in more detail. Therefore, all data including that from the AMMA-CATCH stations were used with a 3-hourly time step, to avoid any resolution effects on the results. To distinguish between the diurnal rainfall peaks, the timing and the size of the rainfall peaks (defined as the mean maximum rainfall amount) are evaluated separately for morning (0000–1200 UTC) and evening (1200–0000 UTC) hours, when the peaks occur.

4. Evaluation results

The West African monsoon season is characterized by large rainfall amounts with substantial diurnal cycles (Fink et al. 2008; Birch et al. 2014). Moreover, the rainfall diurnal cycles vary spatially (He et al. 2015). This tropical rainfall regime poses a challenge for satellite-based precipitation datasets because of its high spatiotemporal variability. In the following, the monsoonal mean rainfall is analyzed and the mean diurnal cycles of rainfall are described. Then, the focus is shifted to the precipitation diurnal cycle variability in the different datasets.

a. Monsoonal mean precipitation

To assess the overall quality of the analyzed datasets, it is useful to validate the monsoonal mean rainfall amounts in comparison with the AMMA-CATCH station data. The monsoonal mean is the mean of the five months (May–September) when the majority of rainfall occurs in West Africa north of 8°N. The results are

TABLE 2. Monsoonal mean precipitation (mm) and relative biases (%) of the analyzed datasets with reference to the AMMA station data during 2000–11 for the Ouémé and Niamey mesosites. Best values are shown in boldface.

	AMMA	TRMM 3B42	TMI	PR	TRMM-COMB	PERSIANN	CMORPH	CMORPH-hq
Ouémé mesosite								
Mean	1051	1018	1153	767	928	1326	1302	1300
Relative bias (%)	—	**−3.1**	+9.7	−27.0	−11.7	+26.2	+23.9	+23.7
Niamey mesosite								
Mean	515	486	423	348	455	1135	719	719
Relative bias (%)	—	**−5.6**	−17.9	−32.4	−11.7	+120.4	+39.6	+39.6

shown in Table 2. There is a negative gradient of rainfall from south to north. The Ouémé mesosite in central Benin (~9.5°N) gets about 1000 mm of rain while the Niamey mesosite (~13.5°N) in southern Niger gets on average 500 mm of rain. Because of different rainfall dynamics (Gosset et al. 2013; Fink et al. 2006), the validation results in Table 2 are shown separately for the Niamey and Ouémé mesosites. The precipitation amounts vary, especially for the Niamey mesosite, where rainfall is less frequent than at the Ouémé mesosite (Gounou et al. 2012); hence single rain events have a large impact on the rain amounts. At the Niamey mesosite the PERSIANN data show more than twice the rainfall amount compared to the ground reference, which is in line with findings by Gosset et al. (2013), while the PR data show the largest underestimations (−27%). For the Ouémé mesosite the monsoonal mean rainfall amounts are in better agreement. The values range from about 750 to 1300 mm with the highest values given by PERSIANN and CMORPH data. An overestimation of CMORPH has also been found by Pierre et al. (2011) in Senegal in West Africa. We find negative biases of the PR product to be on the order of 20%–30%, which is consistent with the negative biases found in convective storms in South America by Rasmussen et al. (2013). Overall, the TRMM 3B42 data are closest to the reference, with deviations of only 5% on average in both analyzed regions.

b. Mean diurnal cycles

The overall monsoonal mean diurnal cycles of rainfall at both mesosites are shown in Fig. 2. At the Ouémé mesosite there is a distinct diurnal cycle with a maximum of rainfall in the evening at around 1800 UTC and a minimum in the morning at about 0800 UTC. A secondary maximum occurs in the early morning at around 0400 UTC. The analyzed satellite datasets reasonably agree with the AMMA-CATCH reference, with a slight tendency toward a delayed peak in the evening. Because of its high temporal resolution, the CMOPRH-hq dataset also nicely captures the secondary peak in the morning. Overall, the rainfall amounts during the evening peak are overestimated by most of the satellite datasets. In terms of the size of the evening peak the three TRMM 3G68 data products substantially deviate from each other, as shown in Fig. 2.

The monsoonal mean diurnal cycle of rainfall is less pronounced at the Niamey mesosite (see Fig. 2). The diurnal cycle as measured by the rain gauges peaks in the morning at about 0600 UTC, and a minimum is observed around noon. During the late evening the rainfall amounts increase again. At the Niamey mesosite the satellite products have more difficulties in capturing the diurnal cycle. It is further obvious that CMORPH, and in particular PERSIANN, overestimate the rainfall while the PR underestimates the rain, as described in the previous subsection. The morning peak is best captured by the CMORPH-hq data but is also visible in the TMI data. Overall, at the Niamey mesosite the satellite products show larger differences from the AMMA-CATCH reference than are seen at the Ouémé mesosite.

c. Year-to-year variability of the diurnal cycle

The monsoonal mean diurnal cycles of rainfall from each of the years from 2000 to 2011 are shown in Figs. 3 and 4 for the Ouémé and Niamey mesosites, respectively. Brief inspection of both figures reveals there are considerable year-to-year variations at both mesosites.

At the Ouémé mesosite, a distinct peak in rainfall during the evening occurs in most of the years (see Fig. 3). An exception is 2004, when the morning peak in rainfall is much more pronounced than is usually the case. The strongest evening peaks are visible in 2005, 2009, and 2010. During 2000–02, the CMORPH and PERSIANN products most strongly overestimate the evening peak. In general, the satellite products are able to capture the year-to-year variations of the diurnal cycles of rainfall. However, a diurnal cycle averaged over only five months has a larger variability and a less smooth diurnal cycle since the number of rainfall events used for averaging is relatively small. In turn, single events might heavily impact this comparison. In PR, TMI, and TRMM-COMB, the deviations are larger, and the peaks are often overestimated. This behavior can most likely be attributed to a limited temporal sampling of the TRMM-only products.

The diurnal cycles during the individual years show larger deviations at the Niamey mesosite compared to the Ouémé mesosite. A prevailing early morning peak of rainfall is observed. Exceptions are the years 2000, 2005, and 2007, when the early morning peak of rainfall hardly exists (see Fig. 4). The most pronounced early morning peaks occurred during 2004 and 2006. Again, the CMORPH-hq data take advantage of the high temporal resolution and can capture much of the observed variability. Overall, PERSIANN tends toward overestimating the results and the TRMM-only products partly show overestimating peaks (e.g., during 2004, 2005, and 2007).

d. Multiyear monthly diurnal cycles

Instead of averaging the diurnal cycles of the five monsoon months [May–September (MJJAS)], as in the previous subsection, we also analyzed the multiyear

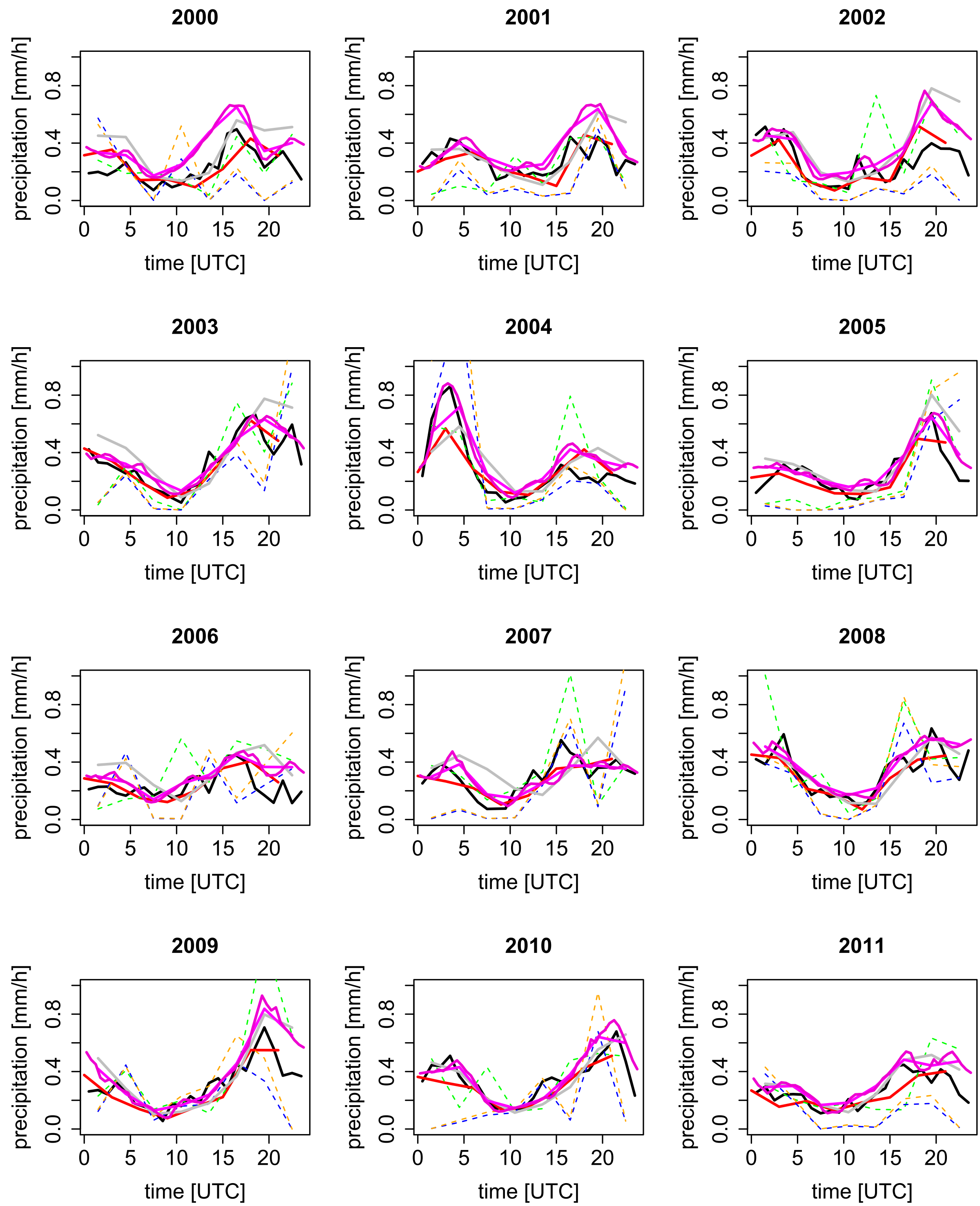

FIG. 3. Annual mean diurnal cycles of the satellite-based datasets and the AMMA-CATCH data at the Ouémé mesosite during the monsoon season (MJJAS) for 2000–11. The key for the lines is provided in Fig. 2.

mean diurnal cycles from month to month. These diurnal cycles of rainfall are presented in Figs. 5 and 6 for the Ouémé and Niamey mesosites, respectively. Additionally, the diurnal cycles of the CLAAS cloud-top temperatures were analyzed during the monsoon months of June–August to give a qualitative measure of the diurnal cloud development alongside of the diurnal rainfall occurrence.

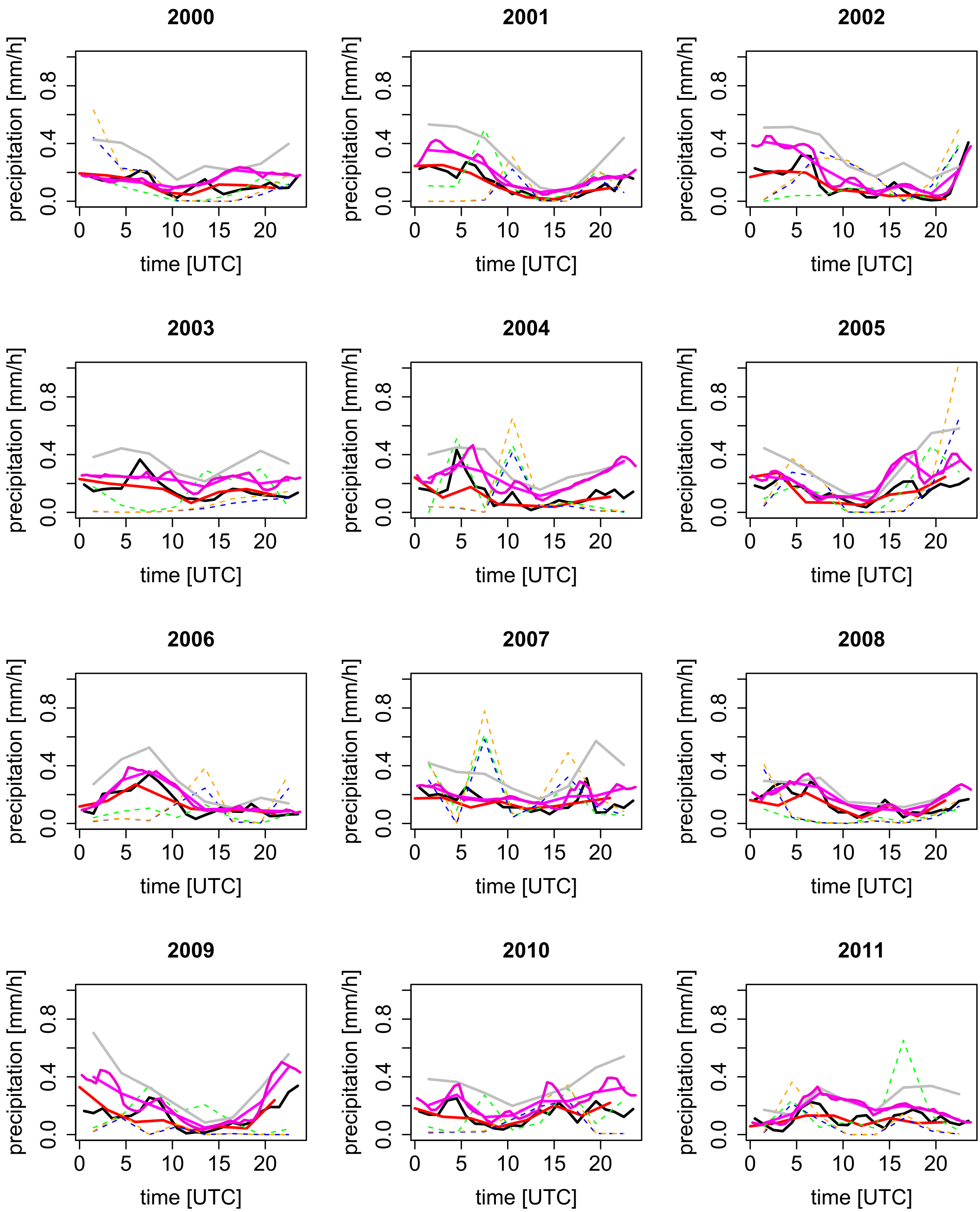

FIG. 4. As in Fig. 3, but for the Niamey mesosite.

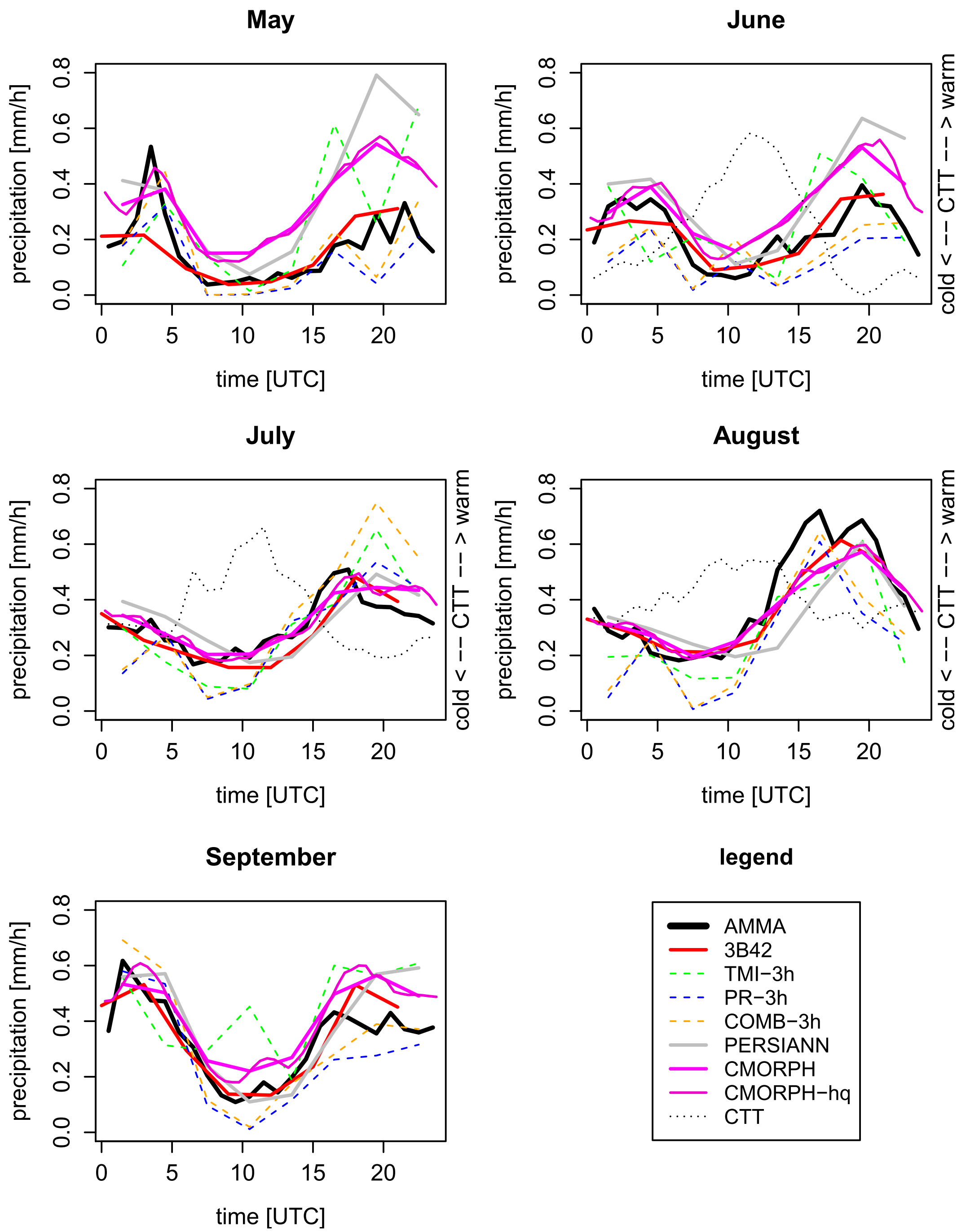

FIG. 5. Multiyear monthly mean diurnal cycles for MJJAS at the Ouémé mesosite, including CTT information for JJA. See legend at the bottom right.

At the Ouémé mesosite we can see that the diurnal cycle substantially varies throughout the monsoon season (cf. Fig. 5). In May there is a distinct peak in the early morning around 0400 UTC while the evening peak is less pronounced. The satellite products show large differences concerning both peaks in terms of rainfall amounts. The early morning peak is underestimated by each of the satellite products, and the evening peak is partly overestimated. The TRMM 3G68 product disagrees with the reference in the evening. In June the diurnal cycle is changing: the early morning peak is weakening and the evening maximum is strengthening relative to the situation in May. In June the satellite datasets agree better with the

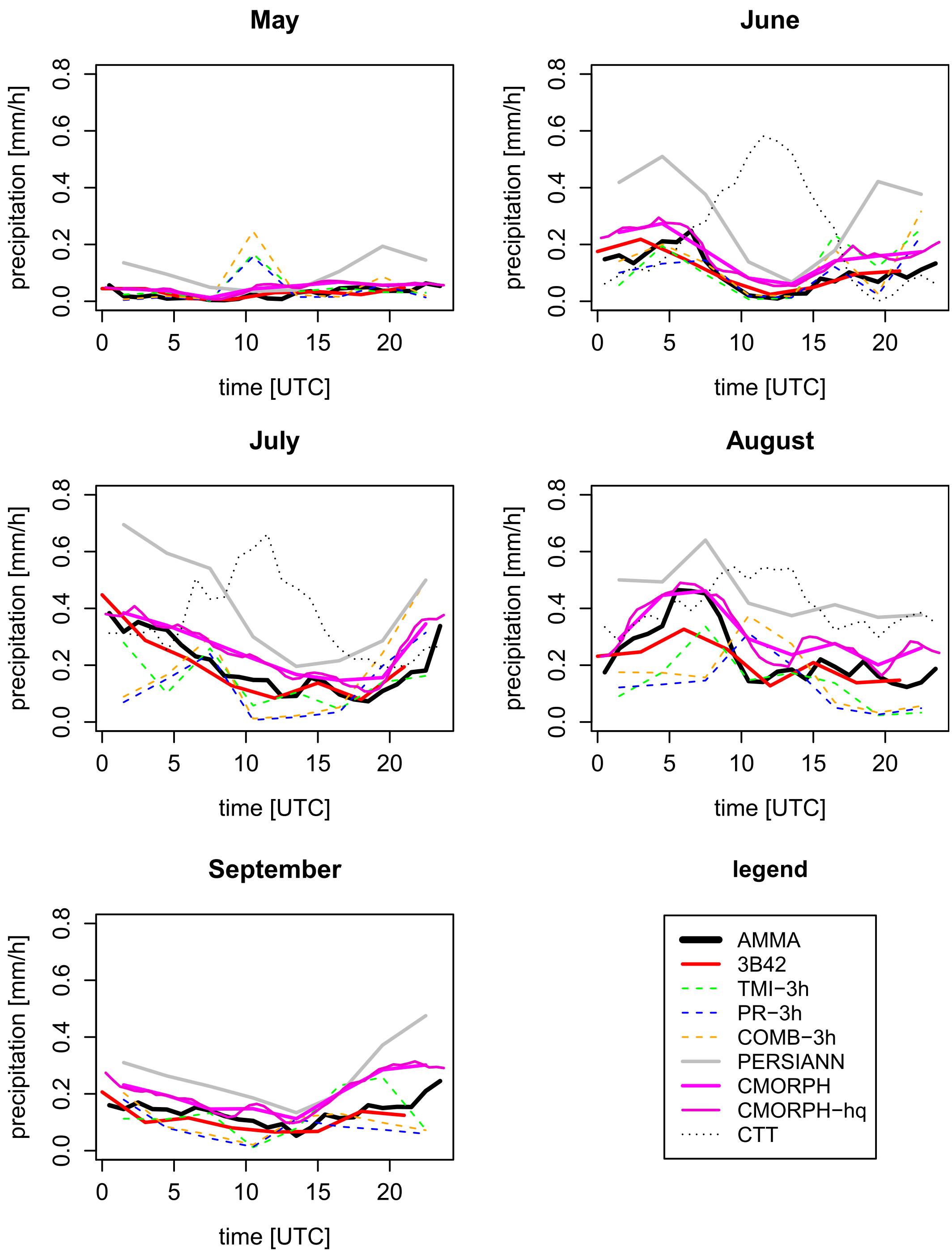

FIG. 6. As in Fig. 5, but for the Niamey mesosite.

AMMA-CATCH reference, while the morning and evening peaks are of approximately the same size. As in May the evening peak is overestimated, especially by PERSIANN and CMORPH. The deviations are smaller during the morning peak. In July the diurnal cycle of rainfall has changed further. There is no more morning peak of rainfall while the evening maximum has strengthened and moved to an earlier time of around 1800 UTC. At this stage of the monsoon we observe the typical characteristic of tropical convection over land that leads to local convective rainfall in the evening as a result of surface heating in an unstable troposphere. Here, we see a slight delay in the time of peak rainfall among almost all of the satellite products (see Fig. 5

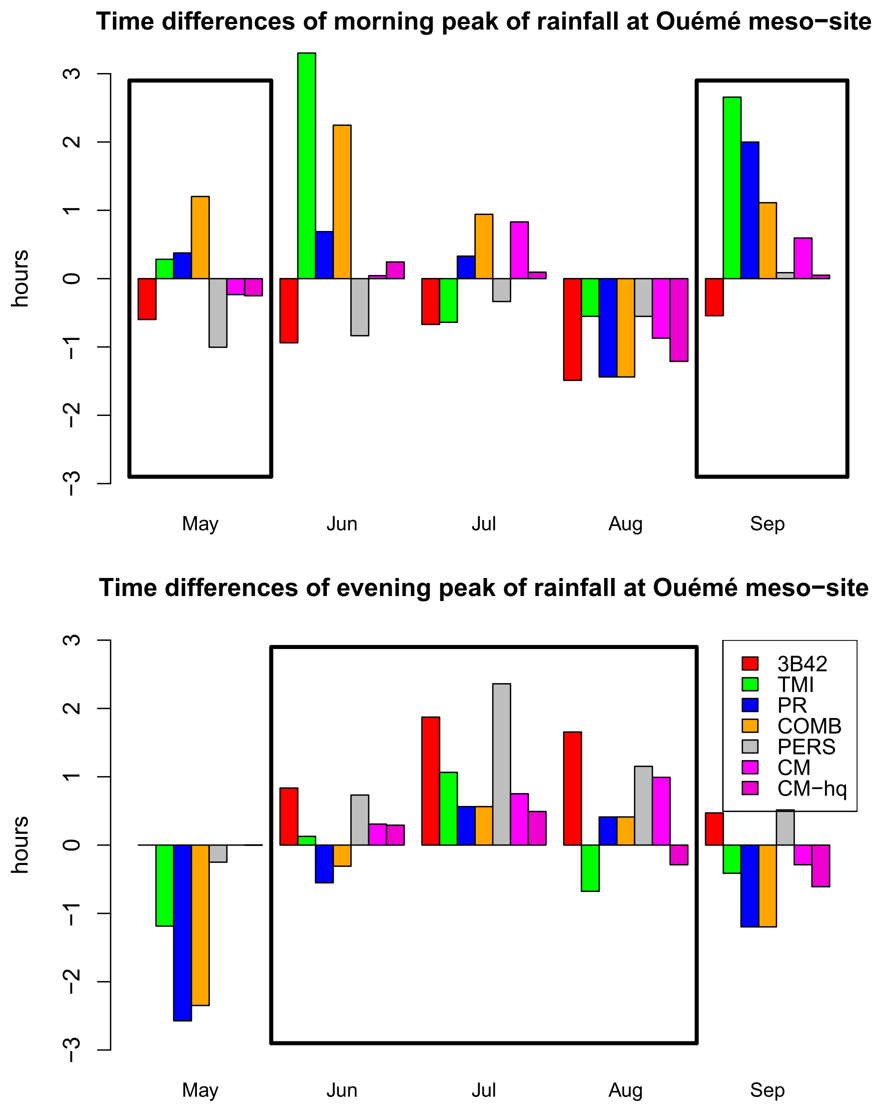

FIG. 7. Time differences (h; satellite data minus station data) in (top) morning and (bottom) evening peaks of monthly mean diurnal rainfall during the monsoon months at the Ouémé mesosite. The most pronounced monthly peaks (morning peaks during MJJAS and evening peaks during JJA) are marked by the black boxes.

and also Fig. 7). This delay corresponds to the minimum in the cloud-top temperature diurnal cycle in July (see black dotted line for CTT in Fig. 5), with the coldest clouds corresponding to the maximum rainfall derived by the satellite products. In August, the diurnal cycles are strongest. Overall, the diurnal cycle is relatively similar to that in July with the exception of a double maximum in the evening. This feature is difficult to interpret and might be attributable to the spatial averaging. Again, most of the satellite datasets are on average slightly late in terms of peak rainfall while the PR and TRMM-COMB peaks coincide with the observations. In September, at the end of the monsoon, the diurnal cycle characteristics are similar to that in May, early in the monsoon, but with a slightly earlier peak.

At the Niamey mesosite the diurnal cycle is also subject to month-to-month variabilities throughout the monsoon (cf. Fig. 6), but the diurnal cycle characteristics are less clear than at the Ouémé mesosite. In May, monsoonal rains are still almost absent at the Niamey site, which is changing in June. Then, the rainfall diurnal cycle characteristics are similar to those seen in Fig. 2 for the overall monsoonal mean diurnal cycle. The maximum rainfall occurs in the morning at around 0700 UTC. PERSIANN strongly overestimates rainfall,

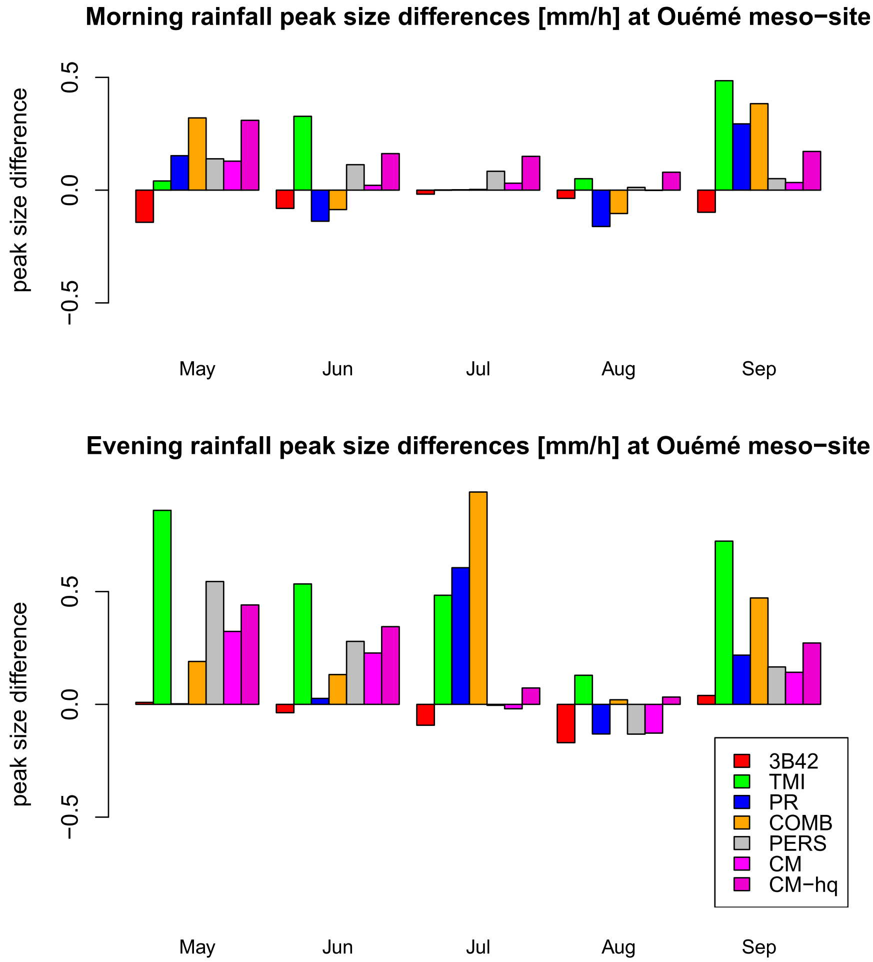

FIG. 8. Size differences (mm h^{-1}; satellite data minus station data) of monthly mean rainfall peaks in the (top) morning and (bottom) evening for the monsoon months at the Ouémé mesosite.

while its timing is reasonable. The early morning peak is captured too early by most of the satellite products, but overall the peak is not very pronounced. The early morning peak is absent in July. There is instead a peak around midnight that the satellite products capture reasonably well. The morning peak appears again in August and is more pronounced than in June. There the PR and TRMM-COMB data deviate most while the TMI data are closer to the reference. At the end of the monsoon, the September rainfall amounts decrease and the diurnal cycle also gets weaker.

The distinct month-to-month variability at the Ouémé mesosite (cf. Fig. 5) is further analyzed in more detail concerning the timing and intensity of the observed morning and evening peaks. Therefore, the AMMA-CATCH data are used at 3-hourly resolution, which is in line with the satellite products (beside CMORPH-hq), to avoid any artificial timing differences. Figure 7 shows the results of the mean morning peaks of rainfall; here, the focus is on the months of May and September, when the morning peak is most distinct (marked by the black boxes in the top part of Fig. 7). While the TRMM 3G68 products capture the morning peaks too late by up to 2 h, the other satellite datasets show only small deviations in the timing of the peak rainfall. Time differences for the evening peak are more systematic during the central monsoon months of June–August, when the evening peak of rainfall dominates on average (see black box in Fig. 7, bottom). June presents a transition month when morning and evening peaks are of similar size. In July and August, when the evening peak is most distinct, a mean delay in the time of maximum rainfall in all the satellite datasets is revealed. This delay is about 1 h on average, with smaller delays seen by the PR, TMI, TRMM-COMB, and CMORPH/CMOPRH-hq datasets. Larger mean delays of up to 2 h are found in the TRMM 3B42 and PERSIANN datasets. Overall, the diurnal timing is captured reasonably well by the satellite datasets while the CMORPH and TRMM-COMB products perform best in identifying the evening peak as observed by the AMMA-CATCH stations.

The differences in the morning and evening peak sizes of rainfall at the Ouémé mesosite are shown in Fig. 8. The morning peaks in May and September are overestimated on average by most of the satellite products. The TRMM 3B42 peak sizes are closest to the AMMA reference. Overall, the overestimations on the mean peak size are on the order of 0.25 mm h^{-1}. The peak size differences in the evening (see Fig. 8, bottom) are larger than those in the morning. Especially in May, June, and September, most of the datasets overestimate the evening rainfall peaks by 0.25–0.5 mm h^{-1}. This results in dominating evening peaks in the satellite datasets, in opposition to the ground-based measurements. In August, when the evening peak is most pronounced, the peak sizes between the satellite and the station data agree well. Owing to its higher temporal resolution, CMORPH-hq shows stronger peaks than does CMORPH.

5. Discussion and conclusions

Rainfall in West Africa is characterized by convective events that are subject to high spatial and temporal variability. It has been shown by Roca et al. (2010) and Gosset et al. (2013) that multisatellite-based precipitation datasets provide valuable information on the daily and subdaily variability of rainfall in West Africa. In this study, it is emphasized that current satellite-based datasets, especially those including geostationary infrared information that get a better temporal coverage, perform reasonably well in capturing the diurnal cycle as observed by ground stations. When averaging over longer time scales, the TRMM-only products (TRMM 3G68) provide reasonable diurnal cycles as well, while care must be taken when short time scales are considered. In this case deviations are larger (see, e.g., Fig. 4), probably as a result of the reduced temporal sampling.

Concerning monsoonal mean rainfall amounts during the time period of 2000–11 the TMPA dataset performs best at both the Niamey and Ouémé mesosites (see Fig. 2), which might be related to the fact that the TMPA product also incorporates gridded rain gauge information on a monthly scale. The overestimations found in CMORPH and PERSIANN, as well as the underestimation by PR, are in line with findings in West Africa by Pierre et al. (2011) and Gosset et al. (2013) for shorter time periods.

The diurnal cycle of rainfall is much more pronounced at the Ouémé mesosite than at the Niamey mesosite. At the latter, maximum diurnal rainfall occurs in the morning hours owing to the arrival of mesoscale convective systems (MCSs). At the Ouémé mesosite we find on average a weaker rainfall peak in the morning and a stronger peak in the evening, in line with the findings of He et al. (2015). These diurnal cycles are subject to interannual variability (see Fig. 3). There are also pronounced variations in the multiyear monthly diurnal cycles throughout the monsoon season. A distinct morning peak in rainfall in May is followed by strong evening peaks of rainfall in July and August, when the locally initiated convective rainfall regime is dominant. In September, things change again with the southward shift of the intertropical convergence zone. These results, based on a 12-yr period, agree well with findings by Fink et al. (2006) during a 1-yr period in 2002.

There also is significant year-to-year variability of the mean diurnal cycle at the Ouémé mesosite, which is expected to be defined by the prevailing precipitation regime being either more MCS dominated or dominated by local convection during the individual years. Nevertheless, the morning and evening peaks exist in most years, with the evening peak dominating the rainfall diurnal cycle. At the Niamey mesosite interannual variability is also present. Owing to large deviations in the diurnal cycles of rainfall (cf. Figs. 6 and 4), which might often be the result of only a few extreme events, a detailed analysis of mean diurnal cycles is not expected to be of much value even when averaging over longer time periods. For more detailed evaluations of rainfall in such an outer tropical regime, it is important to account for sampling uncertainties on spatial and temporal scales. A procedure for how to account for those sampling and algorithm uncertainties within a validation framework has been developed by Roca et al. (2010) and Kirstetter et al. (2013).

Instead, for the Ouémé mesosite the morning and evening peaks in rainfall have been analyzed in more detail as rainfall occurs more frequently. We find that there is a mean time delay of about 1 h in the diurnal rainfall maximum in the evening by most of the satellite datasets (see Fig. 7). A delay in peak rainfall has also been found by Negri et al. (2002a) in the tropics of Brazil. In the PERSIANN dataset this averaged delay is largest, at about 2 h. The TRMM-only products PR, TMI, and TRMM-COMB and the CMORPH dataset show only a minor mean delay. This tendency toward a delay in the timing of the rainfall maximum in the evening can be explained by the use of infrared data in the satellite dataset generation. The infrared algorithms are only sensitive to cloud-top temperatures and convert those into a rain rate. Using cloud-top temperature observations can then lead to a systematically incorrect interpretation of the algorithm by still assuming rainfall, a problem scientists have faced since the early days of satellite imagery interpretation (Reed and Jaffe 1981). Tropical convective precipitation typically occurs during the early stage of convective cloud development, while little precipitation occurs during the later stages when the high and cold ice shield remains (Futyan and Del Genio 2007). The delay in minimum cloud-top temperature with reference to the maximum rainfall peak is especially visible during July and August (see Fig. 5). This might explain why the PERSIANN dataset, which is mainly based on infrared measurements, shows the largest delay in peak precipitation (see Fig. 7). The mean sizes of the morning and evening peaks of rainfall (see Fig. 8) at the Ouémé mesosite are overestimated by most of the satellite datasets. This overestimation is stronger for the evening peak than for the morning peak. This might be related to the prevailing rainfall regimes.

However, the central Benin study region is a good example of where local knowledge of the diurnal and seasonal cycles in the types of convection can be indispensable for interpreting satellite rainfall validation studies. The peak after midnight in the Ouémé mesosite is caused by westward-propagating, organized convective systems (OCSs) that originate from the Jos Plateau and reach the site toward the ends of their lifetimes (Fink et al. 2006). These OCSs develop in high CAPE/CIN and low-level shear environments that prevail during May–June and September near the Ouémé mesosite. In July and especially August, low-shear, low CAPE/CIN, and a moist troposphere favor afternoon convection that is less organized. It can be hypothesized that the observed year-to-year variations in the two diurnal peaks are due to changes in the two convection regimes described above. Moreover, delays in the timing of the later afternoon peak might be related to the fact that this is developing convection whereas the nighttime peak might result from extensive trailing OCS-related anvils. However, this speculation is left for further study. Since the Niamey site only has OCS-type convection (Mathon et al. 2002), the year-to-year variability in the overnight peak is likely related to random changes in the life cycles of the few OCSs that hit Niamey each year. It has been known that the overnight peak is related to OCSs that are triggered near the southern foothills of the Air Mountains in the afternoon hours and propagate at about 50 km h^{-1} toward Niamey in the evening and early night hours (Shinoda et al. 1999).

Overall, the satellite products are able to reasonably capture the diurnal cycles of rainfall and its climatological variability with reference to ground-based rain gauge observations, keeping sampling issues associated with shorter temporal and smaller spatial scales in mind. In particular, the high-resolution CMORPH-hq dataset performs well and allows for more detailed analyses on rainfall diurnal cycles in the tropical regime. The timing of the precipitation diurnal cycles is of great interest among the modeling community. There is the common problem in numerical modeling with reasonably reproducing the precipitation diurnal cycles (Dirmeyer et al. 2012; Birch et al. 2014; Folkins et al. 2014). The applied parameterizations typically generate precipitation too early in the day, while explicitly resolved convection gives more promising results (Fosser et al. 2015). For evaluation, satellite-based precipitation datasets are often used as a reference, especially in regions sparsely covered by rain gauges like the tropics. This study shows the general suitability of selected satellite-based precipitation datasets to reasonably capture the diurnal cycle of precipitation. However, different characteristics are documented for the datasets used with respect to their ability to reproduce the diurnal cycle of precipitation on different spatial and temporal scales. These should be considered when selecting the appropriate datasets for model evaluation and other applications.

Acknowledgments. We thank the EUMETSAT Satellite Application Facility on Climate Monitoring (CM SAF) team for their valuable support. We also thank the data providers for free data access. Thanks go to the AMMA project team for giving access to their database. Author BA acknowledges funding from the Hessian initiative for the development of scientific and economic excellence (LOEWE) at the Biodiversity and Climate Research Centre (BiK-F), Frankfurt am Main. AHF was supported by the DACCIWA project, funded from the European Union Seventh Framework Programme (FP7/2007-2013) under Grant Agreement 603502. We thank the three anonymous reviewers whose comments helped to improve the manuscript.

REFERENCES

Andersson, A., C. Klepp, K. Fennig, S. Bakan, H. Grassl, and J. Schulz, 2011: Evaluation of HOAPS-3 ocean surface freshwater flux components. *J. Appl. Meteor. Climatol.*, **50**, 379–398, doi:10.1175/2010JAMC2341.1.

Ashouri, H., K.-L. Hsu, S. Sorooshian, D. K. Braithwaite, K. R. Knapp, L. D. Cecil, B. R. Nelson, and O. P. Prat, 2015: PERSIANN-CDR: Daily precipitation climate data record from multisatellite observations for hydrological and climate studies. *Bull. Amer. Meteor. Soc.*, **96**, 69–83, doi:10.1175/BAMS-D-13-00068.1.

Bechtold, P., S. Noureddine, L. Philippe, J.-P. Chamboureau, A. Beljaars, and N. Bormann, 2014: Representing equilibrium and nonequilibrium convection in large-scale models. *J. Atmos. Sci.*, **71**, 734–753, doi:10.1175/JAS-D-13-0163.1.

Birch, C. E., D. J. Parker, J. H. Marsham, D. Copsey, and L. Garcia-Carreras, 2014: A seamless assessment of the role of convection in the water cycle of the West African monsoon. *J. Geophys. Res. Atmos.*, **119**, 2890–2912, doi:10.1002/2013JD020887.

Dirmeyer, P. A., and Coauthors, 2012: Simulating the diurnal cycle of rainfall in global climate models: Resolution versus parameterization. *Climate Dyn.*, **39**, 399–418, doi:10.1007/s00382-011-1127-9.

Dobler, A., and B. Ahrens, 2008: Precipitation by a regional climate model and bias correction in Europe and South Asia. *Meteor. Z.*, **17**, 499–509, doi:10.1127/0941-2948/2008/0306.

Ebert, E. E., J. E. Janowiak, and C. Kidd, 2007: Comparison of near-real-time precipitation estimates from satellite observations and numerical models. *Bull. Amer. Meteor. Soc.*, **88**, 47–64, doi:10.1175/BAMS-88-1-47.

Fink, A. H., D. G. Vincent, and V. Ermert, 2006: Rainfall types in the West African Sudanian zone during the summer monsoon 2002. *Mon. Wea. Rev.*, **134**, 2143–2164, doi:10.1175/MWR3182.1.

——, S. Pohle, and R. Hoffmann, 2008: Spatial and temporal rainfall climatologies of Benin. *IMPETUS Atlas Benin. Research Results 2000–2007*, 3rd ed., M. Judex and H.-P. Thamm, Eds., Department of Geography, University of Bonn, Bonn, Germany, 21–22. [Available online at http://doi.pangaea.de/10.1594/PANGAEA.821833.]

Folkins, I., T. Mitovski, and J. R. Pierce, 2014: A simple way to improve the diurnal cycle in convective rainfall over land in climate models. *J. Geophys. Res. Atmos.*, **119**, 2113–2130, doi:10.1002/2013JD020149.

Fosser, G., S. Khodayar, and P. Berg, 2015: Benefit of convection permitting climate model simulations in the representation of convective precipitation. *Climate Dyn.*, **44**, 45–60, doi:10.1007/s00382-014-2242-1.

Futyan, J. M., and A. D. Del Genio, 2007: Deep convective system evolution over Africa and the tropical Atlantic. *J. Climate*, **20**, 5041–5060, doi:10.1175/JCLI4297.1.

Gosset, M., J. Viarre, G. Quantin, and M. Alcoba, 2013: Evaluation of several rainfall products used for hydrological applications over West Africa using two high-resolution gauge networks. *Quart. J. Roy. Meteor. Soc.*, **139**, 923–940, doi:10.1002/qj.2130.

Gounou, A., F. Guichard, and F. Couvreux, 2012: Observations of diurnal cycles over a West African meridional transect: Premonsoon and full-monsoon seasons. *Bound.-Layer Meteor.*, **144**, 329–357, doi:10.1007/s10546-012-9723-8.

Haddad, Z. S., E. A. Smith, C. D. Kummerow, T. Iguchi, M. R. Farrar, S. L. Durden, M. Alves, and W. S. Olson, 1997: The TRMM 'day-1' radar/radiometer combined rain-profiling algorithm. *J. Meteor. Soc. Japan*, **75**, 799–809.

He, X., and Coauthors, 2015: The diurnal cycle of precipitation in regional spectral model simulations over West Africa: Sensitivities to resolution and cumulus schemes. *Wea. Forecasting*, **30**, 424–445, doi:10.1175/WAF-D-14-00013.1.

Huffman, G., and D. T. Bolvin, 2007: The TRMM Multisatellite Precipitation Analysis (TMPA): Quasi-global, multiyear, combined-sensor precipitation estimates at fine scales. *J. Hydrometeor.*, **8**, 38–55, doi:10.1175/JHM560.1.

Janowiak, J. E., V. E. Kousky, and R. J. Joyce, 2005: Diurnal cycle of precipitation determined from the CMORPH high spatial and temporal resolution global precipitation analyses. *J. Geophys. Res.*, **110**, D23105, doi:10.1029/2005JD006156.

Joyce, R., J. Janowiak, P. A. Arkin, and P. Xie, 2004: CMORPH: A method that produces global precipitation estimates from passive microwave and infrared data at high spatial and temporal resolution. *J. Hydrometeor.*, **5**, 487–503, doi:10.1175/1525-7541(2004)005<0487:CAMTPG>2.0.CO;2.

Kidd, C., and V. Levizzani, 2011: Status of satellite precipitation retrievals. *Hydrol. Earth Syst. Sci.*, **15**, 1109–1116, doi:10.5194/hess-15-1109-2011.

Kikuchi, K., and B. Wang, 2008: Diurnal precipitation regimes in the global tropics. *J. Climate*, **21**, 2680–2696, doi:10.1175/2007JCLI2051.1.

Kirstetter, P.-E., N. Viltard, and M. Gosset, 2013: An error model for instantaneous satellite rainfall estimates: Evaluation of BRAIN-TMI over West Africa. *Quart. J. Roy. Meteor. Soc.*, **139**, 894–911, doi:10.1002/qj.1964.

Kniffka, A., M. Stengel, M. Lockhoff, R. Bennartz, and R. Hollmann, 2014: Characteristics of cloud liquid water path from SEVIRI onboard the *Meteosat Second Generation 2* satellite for several cloud types. *Atmos. Meas. Tech.*, **7**, 887–905, doi:10.5194/amt-7-887-2014.

Kothe, S., D. Lüthi, and B. Ahrens, 2014: Analysis of the West African monsoon system in the regional climate model COSMO-CLM. *Int. J. Climatol.*, **34**, 481–493, doi:10.1002/joc.3702.

Kucera, P. A., E. E. Ebert, F. Turk, V. Levizzani, D. Kirschbaum, F. J. Tapiador, A. Loew, and M. Borsche, 2013: Precipitation from space: Advancing Earth system science. *Bull. Amer. Meteor. Soc.*, **94**, 365–375, doi:10.1175/BAMS-D-11-00171.1.

Kummerow, C., W. Barnes, T. Kozu, J. Shiue, and J. Simpson, 1998: The Tropical Rainfall Measuring Mission (TRMM) sensor package. *J. Atmos. Oceanic Technol.*, **15**, 809–817, doi:10.1175/1520-0426(1998)015<0809:TTRMMT>2.0.CO;2.

Lau, W. K. M., K.-M. Kim, and M.-I. Lee, 2007: Characteristics of diurnal and seasonal cycles in global monsoon systems. *J. Meteor. Soc. Japan*, **85A**, 403–416, doi:10.2151/jmsj.85A.403.

Lebel, T., and Coauthors, 2010: The AMMA field campaigns: Multiscale and multidisciplinary observations in the West African region. *Quart. J. Roy. Meteor. Soc.*, **136**, 8–33, doi:10.1002/qj.486.

Mathon, V., H. Laurent, and T. Lebel, 2002: Mesoscale convective system rainfall in the Sahel. *J. Appl. Meteor.*, **41**, 1081–1092, doi:10.1175/1520-0450(2002)041<1081:MCSRIT>2.0.CO;2.

Negri, A. J., R. F. Adler, and L. Xu, 2002a: A TRMM-calibrated infrared rainfall algorithm applied over Brazil. *J. Geophys. Res.*, **107**, 8048, doi:10.1029/2000JD000265.

——, T. L. Bell, and L. Xu, 2002b: Sampling of the diurnal cycle of precipitation using TRMM. *J. Atmos. Oceanic Technol.*, **19**, 1333–1344, doi:10.1175/1520-0426(2002)019<1333:SOTDCO>2.0.CO;2.

Pfeifroth, U., R. Mueller, and B. Ahrens, 2013: Evaluation of satellite-based and reanalysis precipitation data in the tropical Pacific. *J. Appl. Meteor. Climatol.*, **52**, 634–644, doi:10.1175/JAMC-D-12-049.1.

Pierre, C., G. Bergametti, B. Marticorena, E. Mougin, T. Lebel, and A. Ali, 2011: Pluriannual comparisons of satellite based rainfall products over the Sahelian belt for seasonal vegetation modeling. *J. Geophys. Res.*, **116**, D18201, doi:10.1029/2011JD016115.

Pohl, B., M. Rouault, and S. S. Roy, 2014: Simulation of the annual and diurnal cycles of rainfall over South Africa by a regional climate model. *Climate Dyn.*, **43**, 2207–2226, doi:10.1007/s00382-013-2046-8.

Rasmussen, K. L., S. L. Choi, M. D. Zuluaga, and R. A. Houze Jr., 2013: TRMM precipitation bias in extreme storms in South America. *Geophys. Res. Lett.*, **40**, 3457–3461, doi:10.1002/grl.50651.

Reed, R. J., and K. D. Jaffe, 1981: Diurnal variation of summer convection over West Africa and the tropical eastern Atlantic during 1974 and 1978. *Mon. Wea. Rev.*, **109**, 2527–2534, doi:10.1175/1520-0493(1981)109<2527:DVOSCO>2.0.CO;2.

Roca, R., P. Chambon, I. Jobard, P.-E. Kirstetter, M. Gosset, and J. C. Bergès, 2010: Comparing satellite and surface rainfall products over West Africa at meteorologically relevant scales during the AMMA campaign using error estimates. *J. Appl. Meteor. Climatol.*, **49**, 715–731, doi:10.1175/2009JAMC2318.1.

Sane, Y., and Coauthors, 2012: An analysis of the diurnal cycle of precipitation over Dakar using local rain-gauge data and a general circulation model. *Quart. J. Roy. Meteor. Soc.*, **138**, 2182–2195, doi:10.1002/qj.1932.

Sapiano, M. R. P., and P. A. Arkin, 2009: An intercomparison and validation of high-resolution satellite precipitation estimates with 3-hourly gauge data. *J. Hydrometeor.*, **10**, 149–166, doi:10.1175/2008JHM1052.1.

Sato, T., H. Miura, M. Satoh, Y. N. Takayabu, and Y. Wang, 2009: Diurnal cycle of precipitation in the tropics simulated in a global cloud-resolving model. *J. Climate*, **22**, 4809–4826, doi:10.1175/2009JCLI2890.1.

Shinoda, M., T. Okatani, and M. Saloum, 1999: Diurnal variations of rainfall over Niger in the West African Sahel: A comparison between wet and drought years. *Int. J. Climatol.*, **19**, 81–94, doi:10.1002/(SICI)1097-0088(199901)19:1<81::AID-JOC350>3.0.CO;2-F.

Sorooshian, S., K.-l. Hsu, X. Gao, H. V. Gupta, B. Imam, and D. Braithwaite, 2000: Evaluation of PERSIANN system satellite-based estimates of tropical rainfall. *Bull. Amer. Meteor. Soc.*, **81**, 2035–2046, doi:10.1175/1520-0477(2000)081<2035:EOPSSE>2.3.CO;2.

Stengel, M. S., A. K. Kniffka, J. F. M. Meirink, M. L. Lockhoff, J. T. Tan, and R. H. Hollmann, 2014: CLAAS: The CM SAF cloud property data set using SEVIRI. *Atmos. Chem. Phys.*, **14**, 4297–4311, doi:10.5194/acp-14-4297-2014.

Tapiador, F. J., and Coauthors, 2012: Global precipitation measurement: Methods, datasets and applications. *Atmos. Res.*, **104–105**, 70–97, doi:10.1016/j.atmosres.2011.10.021.

Yang, G.-Y., and J. Slingo, 2001: The diurnal cycle in the tropics. *Mon. Wea. Rev.*, **129**, 784–801, doi:10.1175/1520-0493(2001)129<0784:TDCITT>2.0.CO;2.